Check for updates

ADVANCING EARTH AND SPACE SCIENCE

Geophysical Research Letters

RESEARCH LETTER
10.1029/2022GL100703

Key Points:

- Robust, skillful precipitation reconstruction of the Kabul River Basin from tree rings
- Steady decline in the low end of the precipitation distribution implies increasing drought risks
- Prolonged droughts are being replaced by shorter, more frequent ones, interspersed with more frequent pluvials

Supporting Information:

Supporting Information may be found in the online version of this article.

Correspondence to:

H. T. T. Nguyen and P. Cherubini,
hnguyen@ldeo.columbia.edu;
paolo.cherubini@wsl.ch

Citation:

Khan, N., Nguyen, H. T. T., Galelli, S., & Cherubini, P. (2022). Increasing drought risks over the past four centuries amidst projected flood intensification in the Kabul River Basin (Afghanistan and Pakistan)—Evidence from tree rings. *Geophysical Research Letters*, *49*, e2022GL100703. https://doi.org/10.1029/2022GL100703

Received 4 AUG 2022
Accepted 11 NOV 2022

Author Contributions:

Conceptualization: Nasrullah Khan, Hung T. T. Nguyen, Paolo Cherubini
Data curation: Nasrullah Khan
Formal analysis: Nasrullah Khan, Hung T. T. Nguyen
Funding acquisition: Paolo Cherubini
Investigation: Nasrullah Khan, Hung T. T. Nguyen
Methodology: Nasrullah Khan, Hung T. T. Nguyen
Resources: Nasrullah Khan
Software: Hung T. T. Nguyen

© 2022. The Authors.
This is an open access article under the terms of the Creative Commons Attribution-NonCommercial-NoDerivs License, which permits use and distribution in any medium, provided the original work is properly cited, the use is non-commercial and no modifications or adaptations are made.

Increasing Drought Risks Over the Past Four Centuries Amidst Projected Flood Intensification in the Kabul River Basin (Afghanistan and Pakistan)—Evidence From Tree Rings

Nasrullah Khan[1,2], Hung T. T. Nguyen[3], Stefano Galelli[3,4], and Paolo Cherubini[2,3,5]

[1]Department of Botany, University of Malakand, Chakdara, Pakistan, [2]WSL Swiss Federal Institute for Forest, Snow and Landscape Research, Birmensdorf, Switzerland, [3]Tree Ring Laboratory, Lamont-Doherty Earth Observatory, Columbia University, Palisades, NY, USA, [4]Pillar of Engineering Systems and Design, Singapore University of Technology and Design, Singapore, Singapore, [5]Faculty of Forestry, University of British Columbia, Vancouver, BC, Canada

Abstract Increased flood risks have been projected, but with large uncertainties, in the Kabul River Basin (Afghanistan and Pakistan). To place future changes in a long-term perspective, we produce a 382-year precipitation reconstruction for the basin using seven tree-ring chronologies of old-growth conifers from the Hindu Kush Mountains, a monsoon-shadow area. The reconstruction proves robust over rigorous cross-validations ($R^2 = 0.60$, RE = 0.60, CE = 0.53). The full reconstruction (1637–2018) reveals a steady decline in the low end of the precipitation distribution, implying increasing drought risks. We show that droughts are getting more severe, shorter, and more frequent, interspersed with more frequent pluvials in the past century. Drought risks, compounded with projected flood intensification, pose significant threats for this transboundary river. Therefore, future water management needs to account for both flood and drought risks and be informed by long-term hydroclimatic variability.

Plain Language Summary The Kabul River is a transboundary river spanning eastern Afghanistan and northern Pakistan. It is an important tributary of the Indus, one of the world's largest rivers with intensive water withdrawals for human use. With climate change, the Kabul River is projected to have more frequent and larger floods, but the projections are very uncertain. To have a better understanding of these future projections, we need to look at how the region's climate has changed in the past. Tree rings are a valuable source of information to serve that need. Using old-growth conifers from the Hindu Kush Mountains, western Himalaya, we reconstruct four centuries of precipitation (rainfall) history for the Kabul River Basin. From the reconstruction, we observe that dry years are getting drier. Thus, the risks of severe droughts are increasing. Prolonged droughts are being replaced by shorter but more frequent ones, and periods of sustained high precipitation are also becoming more frequent. When seen in combination with earlier reports, our results imply that the Kabul River Basin is facing both floods and drought risks, and these are significant threats to the water security of the basin.

1. Introduction

The Indus River system is one of the largest basins in the world (Best, 2019). Yet, owing to the extensive human-made water storage and withdrawal infrastructure along its course, the river is nearly depleted (Sharma et al., 2010). Shared by four countries—Pakistan, Afghanistan, China, and India—the basin supports a population of about 300 million people (Laghari et al., 2012). Among these, the semi-arid countries of Afghanistan and Pakistan are particularly reliant on the Indus, and are facing acute water and food shortages as well as threats of transboundary water conflicts (Akhtar & Iqbal, 2017; Atef et al., 2019). Located in the Indus headwaters, and originated from the Hindu Kush–Karakoram Mountains, the Kabul River is an important tributary of the Indus, accounting for about 10% of the annual flow and supplying water directly to the Afghan capital, Kabul (Lashkaripour & Hussaini, 2008). The Kabul River has experienced intensive human-induced environmental changes in the last 40-years (Ahmadullah & Dongshik, 2015), and new dams are planned to be built (Yousaf, 2017). Development in both the Afghanistan's and Pakistan's sides of the river, such as dam construction and increase in built-up and cultivated areas, may worsen transboundary water conflicts (Akhtar & Iqbal, 2017; Atef et al., 2019; Taraky et al., 2021).

19448007, 2022, 24, Downloaded from https://agupubs.onlinelibrary.wiley.com/doi/10.1029/2022GL100703 by Schweizerische Akademie Der, Wiley Online Library on [29/12/2022]. See the Terms and Conditions (https://onlinelibrary.wiley.com/terms-and-conditions) on Wiley Online Library for rules of use; OA articles are governed by the applicable Creative Commons License

19448007, 2022, 24, Downloaded from https://agupubs.onlinelibrary.wiley.com/doi/10.1029/2022GL100703 by Schweizerische Akademie Der, Wiley Online Library on [29/12/2022]. See the Terms and Conditions (https://onlinelibrary.wiley.com/terms-and-conditions) on Wiley Online Library for rules of use; OA articles are governed by the applicable Creative Commons License

Supervision: Stefano Galelli, Paolo Cherubini
Validation: Hung T. T. Nguyen, Stefano Galelli, Paolo Cherubini
Visualization: Nasrullah Khan, Hung T. T. Nguyen
Writing – original draft: Nasrullah Khan, Hung T. T. Nguyen, Stefano Galelli, Paolo Cherubini
Writing – review & editing: Nasrullah Khan, Hung T. T. Nguyen, Stefano Galelli, Paolo Cherubini

On top of the increasing water stresses due to human activities, the Kabul River Basin faces an uncertain future because of climate change. Climate models predict consistent warming and drying trends in the Indus Basin, but with considerable uncertainties surrounding the magnitude and spatial pattern of these changes (Shakir et al., 2010; Wi et al., 2015; Z. Ahmad et al., 2012). Despite the overall projected drying trend in the Indus Basin, little change has been observed in annual precipitation in the Indus headwaters over the past decades (Khattak et al., 2011), and most climate models project an increase in precipitation in the Kabul River particularly (Iqbal et al., 2018). The combination of higher precipitation and enhanced snowmelt due to warming is thus projected to increase flood frequency and intensity in the Kabul River Basin (Iqbal et al., 2018; S. Ahmad et al., 2021).

A major factor that confounds projections of water resources availability in the region is a peculiar phenomenon named the "Karakoram Anomaly," where glaciers in the Karakoram Mountains gain masses and experience higher frequencies of glacial surges, contradicting the overall trends in High-Mountain Asia and other glaciated regions worldwide (Hewitt, 2005). The cause of this anomaly remains undetermined, although several plausible causes have been put forth (see e.g., Farinotti et al., 2020; Forsythe et al., 2017; Kapnick et al., 2014; Yao et al., 2012). Furthermore, while evidence from tree rings suggests that the anomaly may have been stable for centuries (Zafar et al., 2016), the future stability of the phenomenon is highly uncertain with global warming (Farinotti et al., 2020). As the Indus derives a significant amount of runoff from the Karakoram Mountains, these uncertainties greatly hamper the assessment of future surface water availability in the region.

Against this back drop of increasing water stress and uncertain hydroclimatic projections, we turn our attention to the past hydroclimatic variability of the Kabul River Basin. This knowledge could help constraint future projections and put recent and future changes in a long-term perspective. Here, we present a four-century annual precipitation reconstruction for the Kabul River Basin using seven old-growth conifer chronologies developed from both the Afghanistan's and Pakistan's sides of the basin. Our reconstruction provides a long-term record of moisture input to the basin—an important step towards understanding the long-term changes in the water cycle and their implications to regional water management.

2. Materials and Methods

2.1. Study Area and Sampled Species

We sampled three coniferous species on the Hindu Kush Mountains (Figures 1a and 1b): *Cedrus deodara* (commonly known as Himalayan cedar), *Picea smithiana* (Himalayan spruce) and *Pinus gerardiana* (Chilgoza pine). Six of the sites were first sampled in 2005–2006 (Khan et al., 2008; Ahmed et al., 2011; Cook et al., 2013) and here we updated them to 2018 using micro-cores from the same living trees that were tagged in previous field campaigns. We also developed one new site (Lowari Top). Details of the sites are provided in Table S1.

P. gerardiana is typically found in the inner semi-arid regions of the north-western Himalaya, between 1,800 and 3,000 m asl (Singh et al., 2021), with low summer monsoon rainfall but high winter snowpack. *C. deodara* is found through the western Himalayas at elevations between 1,500 and 3,300 m asl. This species forms mixed stands with *P. smithiana* at 2,500 m and above, whereas at lower elevations, it usually forms associations with *Abies pindrow* and *Pinus wallichiana* (Champion et al., 1965). *C. deodara* generally prefers sites with low humidity and high winter snowpack (Raizada & Sahni, 1960; Sahni, 1990). In the study area, the three species were found growing on steep rocky slopes with thin soil cover in Chitral Gol National Park, Bumburat Kalash valley, and Lowari Top (Pakistan), and Nuristan Province (Afghanistan) (Figures 1a and 1b). All three species grow in open stands; this might be due to long-term anthropogenic interventions, as the local communities depend on these forests (N. Khan et al., 2013). As a result, tree-ring patterns of the sampled trees should not be influenced much by stand dynamics such as inter-tree competition.

2.2. Tree Ring Data

During the sampling phase, care was taken to select healthy trees without visible injuries or fire scars. Cores were sampled at breast height (1.3 m), dried, glued, and sanded following standard dendrochronological protocols. Samples were cross-dated with the skeleton plot method (Speer, 2010; Stokes & Smiley, 1996) and measured with a LINTAB tree-ring measurement station (Rinntech, Heidelberg Germany). Measurements were then statistically validated using the software COFECHA (Holmes, 1983).

10.1029/2022GL100703

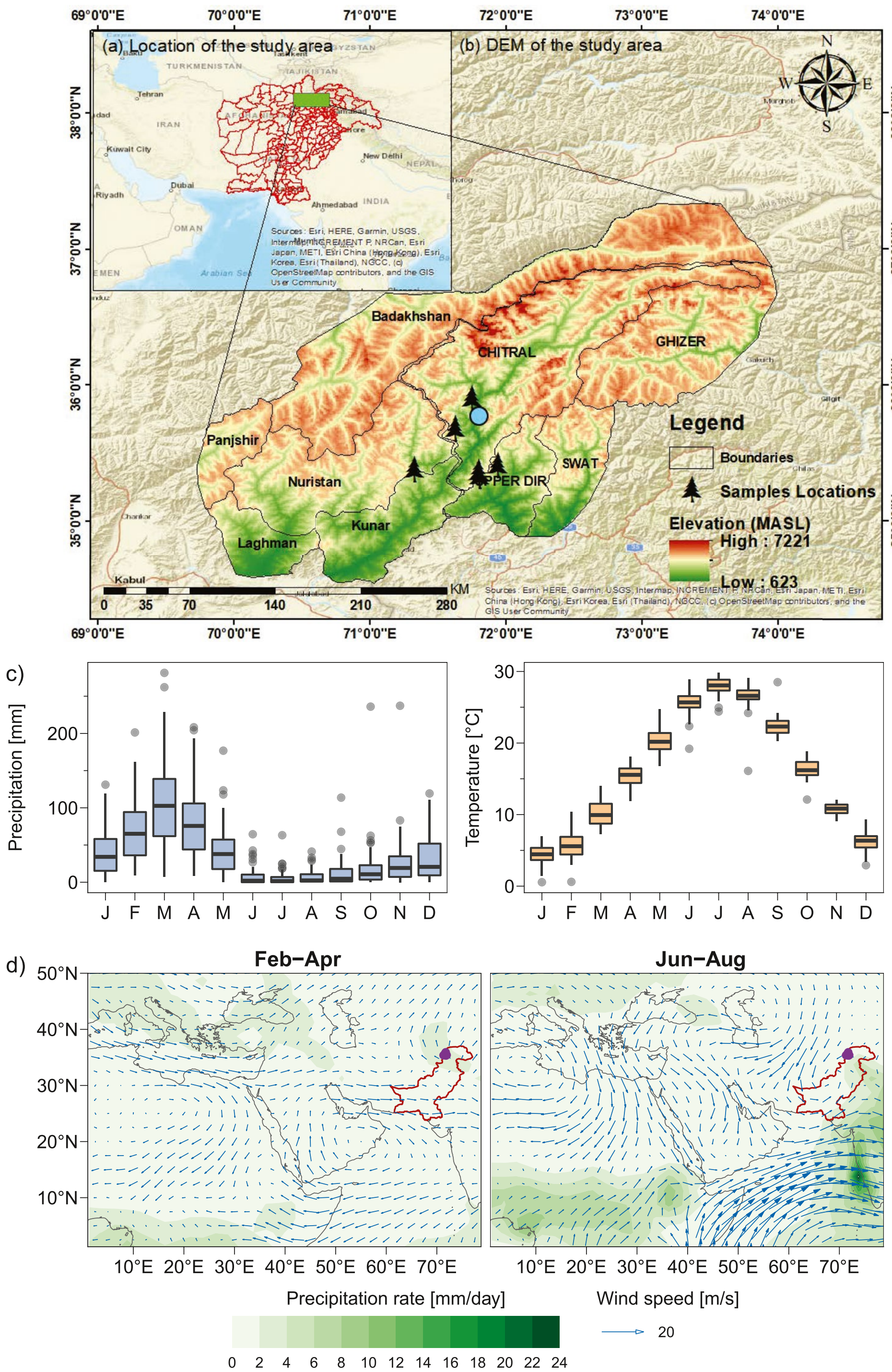

Figure 1. (a) Location of the study region. (b) Map of the study area showing the sampling sites, Chitral meteorological station (blue dot), as well as the topography. (c) Monthly distribution of precipitation and temperature at Chitral. (d) Visualization of moisture transport to our study site, created by overlaying 850 hPa winds on gridded precipitation, averaged for the period 1979–2021. Pakistan is highlighted in red and the study site in purple. During February–April, note the westerly winds from the Mediterranean Sea. During June–August, note that the study site is located away from monsoon winds and receives little rain. Wind data from NCEP-DOE Reanalysis (Kanamitsu et al., 2002) and precipitation data from GPCP (Adler et al., 2018).

19448007, 2022, 24, Downloaded from https://agupubs.onlinelibrary.wiley.com/doi/10.1029/2022GL100703 by Schweizerische Akademie Der, Wiley Online Library on [29/12/2022]. See the Terms and Conditions (https://onlinelibrary.wiley.com/terms-and-conditions) on Wiley Online Library for rules of use; OA articles are governed by the applicable Creative Commons License

We detrended and standardized the chronologies using the program ARSTAN (Cook, 1985). We found that our samples did not follow the negative exponential or Hugershoff growth curves, likely because these forests are logged by the local communities (Section 2.1). To account for these disturbances, a data-adaptive detrending method is more suitable. By experimenting we found that the Friedman variable span smoother worked well, and yielded the highest $\bar{r}$ values (Table S2 in Supporting Information S1). In a few cases where the Friedman smoother showed a lack of fit, the cubic smoothing spline (Cook & Peters, 1981) was used.

For each site, the program ARSTAN produces three chronologies: standard, residual, and ARSTAN. The standard chronology is obtained by averaging all tree ring indices (detrended tree ring time series) at a site. When the tree ring indices have significant autocorrelations that violate the weak stationarity assumption, they must be pre-whitened before averaging; this yields the residual chronology (Cook & Kairiukstis, 1990). However, when the target climate variable has a significant autocorrelation structure, the residual chronology, having been pre-whitened, may fail to reproduce such autocorrelations. As a result, the ARSTAN chronology is introduced (Cook, 1985), where the residual chronology is "re-reddened": a common autocorrelation structure is pooled from all tree ring indices and added back to the residual chronology. In our particular case, the precipitation data show no significant autocorrelation (Figure S1 in Supporting Information S1); therefore, we selected the residual chronologies instead of the ARSTAN ones. Upon further verification, we found that indeed the reconstruction using the ARSTAN chronologies, holding all else equal, has much lower skills than that obtained with the residual chronologies (Table S3 in Supporting Information S1).

The final chronologies and their subsample signal strength (SSS; Wigley et al., 1984) are shown in Figure S2 in Supporting Information S1, and other statistics are reported in Table S4 in Supporting Information S1. Following recommendations by Buras (2017), we used SSS rather than the expressed population signal to determine the length of chronology to retain. The SSS was computed using the R package `dplR` (Bunn, 2008). Wigley et al. (1984) recommended a threshold of 0.85 (and this is the value commonly used in the literature); however, they noted that it was only a guideline. Here, in order to maximize the useable length of tree ring data, we chose a threshold of 0.75, at which point the chronologies still appear stable (Figure S2 in Supporting Information S1). Sensitivity analyses (Figure S3 and Table S5 in Supporting Information S1) show that this choice does not affect the results.

2.3. Climate Data

We obtained monthly precipitation and temperature data for the Chitral meteorological station (Figure 1b). Our record covers the period 1965–2018, among the longest records in Pakistan. Precipitation peaks in March, and the wet season spans from December to May, contributing more than 70% of the total annual precipitation (Figure 1c). June to August are usually the driest months. As temperatures are mostly above freezing, precipitations are typically in liquid form. Our study region is located in a monsoon shadow area, away from summer monsoon winds, and precipitation is predominantly delivered by western disturbances originating from the Mediterranean Sea (Figure 1d; cf., Iqbal et al., 2018; Ridley et al., 2013).

2.4. Climate–Growth Relationship

To determine the target reconstruction season, we calculated the correlations between each chronology and the precipitation of each month from prior year's January to current year's December (Figure 2). All sites display a generally consistent correlation pattern between tree ring widths and precipitation, with stronger correlations observed between January and May, during the wet season. Highest correlations values are above 0.5, observed in March, April, and May at the CDBK, PGBK, CDNA sites, respectively. Several sites (e.g., CDBK and PGCG) also correlate significantly with precipitation in the shoulder months (September to December). Based on these results, we chose the full water year (September to August) as the reconstruction target. Reconstructing the water year precipitation provides the total annual moisture input to the basin, which is potentially useful for hydrological modeling and water management applications.

2.5. Reconstruction Procedure

We performed principal component analysis (PCA) to account for multicollinearity. However, PCA could not be implemented directly because the chronologies start and end at different times, leaving data gaps. Therefore, we first imputed the data gaps using the R package `missMDA` (Josse & Husson, 2016). The imputation procedure

19448007, 2022, 24, Downloaded from https://agupubs.onlinelibrary.wiley.com/doi/10.1029/2022GL100703 by Schweizerische Akademie Der, Wiley Online Library on [29/12/2022]. See the Terms and Conditions (https://onlinelibrary.wiley.com/terms-and-conditions) on Wiley Online Library for rules of use; OA articles are governed by the applicable Creative Commons License

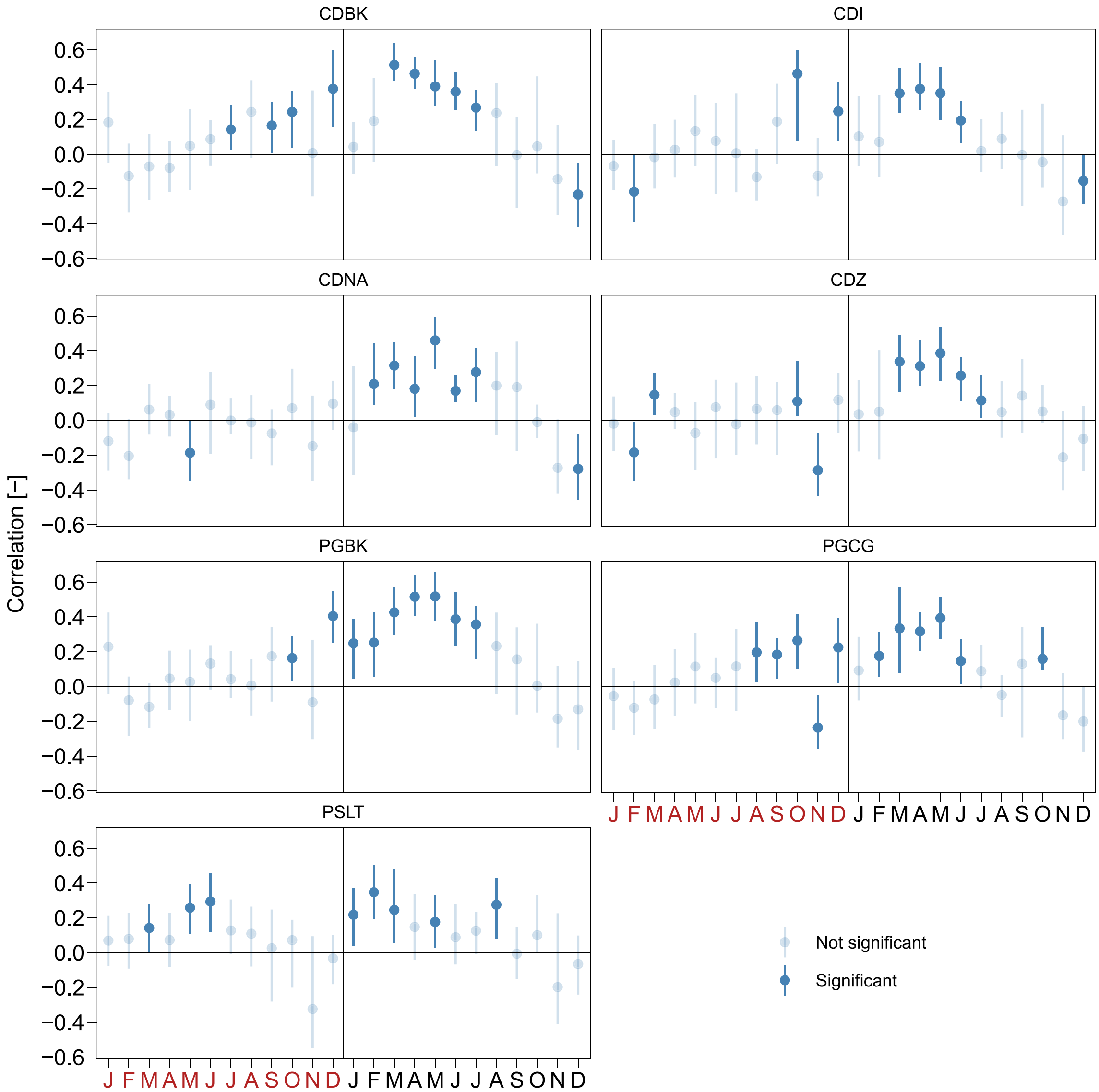

Figure 2. Correlations between each tree ring chronology and monthly precipitation at Chitral from prior year's January to current year's December. Correlations are bootstrapped 1,000 times using the stationary bootstrap (Politis & Romano, 1994). The dots are the median and the line ranges are the 5%–95% quantiles of the bootstrap replicates. Correlations that are not statistically significant ($\alpha = 0.05$) are faded. The months of the prior year are labeled in red.

iteratively fills the data gaps until the principal components (PCs) obtained from the gap filled data converge to those of the observed data. This gap filling strategy has been implemented with good results in earlier reconstruction works (e.g., Nguyen et al., 2021, 2022; Stagge et al., 2018). The results of the gap filling procedure are shown in Figure S4 in Supporting Information S1.

After gap filling, we conducted the final PCA (details in Figure S5 in Supporting Information S1). Only PC1 has an eigenvalue greater than one, but PC2 and PC3's eigenvalues are very close to one (0.98 and 0.89, respectively). Therefore, PC2 and PC3 were also considered candidate predictors. We then carried out backward stepwise linear regression, which resulted in PC1 and PC2 being retained in the final model.

The reconstruction was cross-validated with a moving-block cross-validation procedure, in which contiguous, rolling blocks of k years were left out for verification while the model was calibrated with the remaining data (Nguyen et al., 2020; Higgins et al., 2022). Here, k was set as 14 years, or 25% of the data length. This choice leaves sufficient calibration data (40 years) while still being able to assess the model's predictive skills on a

19448007, 2022, 24, Downloaded from https://agupubs.onlinelibrary.wiley.com/doi/10.1029/2022GL100703 by Schweizerische Akademie Der, Wiley Online Library on [29/12/2022]. See the Terms and Conditions (https://onlinelibrary.wiley.com/terms-and-conditions) on Wiley Online Library for rules of use; OA articles are governed by the applicable Creative Commons License

19448007, 2022, 24, Downloaded from https://agupubs.onlinelibrary.wiley.com/doi/10.1029/2022GL100703 by Schweizerische Akademie Der, Wiley Online Library on [29/12/2022]. See the Terms and Conditions (https://onlinelibrary.wiley.com/terms-and-conditions) on Wiley Online Library for rules of use; OA articles are governed by the applicable Creative Commons License

decadal time scale. The commonly used metrics reduction of error (RE) and coefficient of efficiency (CE) (Cook & Kairiukstis, 1990; Nash & Sutcliffe, 1970) were used to assess the reconstruction quality.

Finally, the reconstructed time series was bias-corrected using the quantile mapping method from the R package `qmap` (Gudmundsson, 2016; Robeson et al., 2020). This step is important to ensure that the instrumental period's portion of the reconstruction has a similar distribution to that of the instrumental data. If the distributions were not matched, subsequent statistical comparisons between the paleo and instrumental periods would not be fair.

2.6. Trend and Drought/Pluvial Analyses

We used quantile regression (Koenker, 2005; Maxwell et al., 2021) to analyze the trends in different parts of the precipitation distribution. The 1st, 5th, 50th (median), 95th, and 99th percentiles are regressed against time to examine how the bulk and extremes of the precipitation distribution have changed over a long term.

For the purpose of drought and pluvial analysis, we define a meteorological drought event as one that starts with two consecutive years of negative precipitation anomalies, and ends with two consecutive years of positive anomalies (two-start two-end; cf. Coats et al., 2013; Herweijer et al., 2007). The last 2 years with positive anomalies are not counted toward the drought duration. Anomalies are calculated with respect to the mean precipitation over the full reconstruction (1637–2018). A drought's magnitude is taken as the largest precipitation anomaly during its duration. The same two-start two-end definition is applied for pluvial episodes where the signs of the anomalies are reversed.

3. Results

3.1. Model Performance

The mean performance scores of the reconstruction across 30 cross-validation runs are: $R^2 = 0.60$, RE = 0.60, and CE = 0.53. In all cross-validation runs, RE and CE are always positive (Figure S6 in Supporting Information S1). The reconstruction explains 60% of variance in precipitation, and the model shows robustly good skills under a rigorous cross-validation scheme. This is also reflected by the reconstruction trajectory, which matches observation closely (Figure 3a). However, agreement between the reconstruction and observations is not as good in the extremes, particularly in the wettest years. This leads to a mismatch between the density of the reconstruction and that of the instrumental data (Figure 3b): frequencies of extremely dry and extremely wet years are underestimated by the reconstruction. This is a common limitation of tree-ring-based reconstructions (see e.g., Robeson et al., 2020). There are two possible causes: first, the climate–growth relationship may become

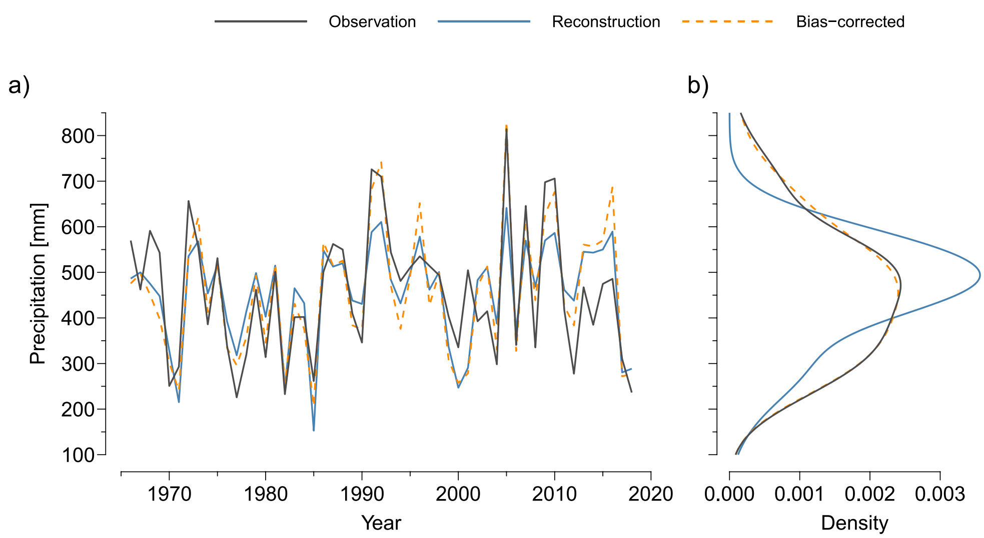

Figure 3. (a) Comparison between observed, reconstructed, and bias-corrected water-year precipitation time series for the instrumental period (1965–2018). (b) Comparison between the densities of observed, reconstructed, and bias-corrected water year precipitation. All densities are calculated for the instrumental period only.

nonlinear at the extremes (Torbenson & Stagge, 2021); and second, trees may not be able to capture moisture inputs beyond the soil saturation level (Meko & Graybill, 1995; Nguyen et al., 2021). These shortcomings can be mitigated by bias correction. We found that the bias-corrected precipitation distribution matches very closely with observations, much better than the uncorrected distribution does (Figure 3b).

3.2. Four Centuries of Precipitation Variability

In the full reconstruction (Figure 4a), we observed periods of high and low variability. Notably, the period 1820–1920 has lower variability than other 100-year periods. There are two clusters of extremely wet years (above 95th percentile): 1650–1700 and 1925–1950, and a cluster of extremely dry years (below 5th percentile) between 1775 and 1825. We observed upward trends in median and high precipitations (50th–95th percentiles), but these trends are not statistically significant, likely due to the large fluctuations in the upper part of the distribution. There are, however, significant and considerable downward trends in low precipitations (first percentile: −0.22 mm/year; fifth percentile: −0.12 mm/year). Overall, the 1st–99th percentile range had widened between 1637 and 2018, suggesting that the water cycle had been intensified, with more statistically significant intensification on the low extreme. It is also important to note that despite this intensification, the instrumental period (1964–2018) contains neither the driest nor the wettest year on record. The lowest measured precipitation (in 1977) is 226 mm while the lowest reconstructed precipitation is 202 mm, in 1815. The highest measured precipitation (814 mm, in 2005) was exceeded four times in the pre-instrumental period (1661: 889 mm; 1804: 878 mm; 1924: 857 mm; and 1930: 817 mm). This suggests that the minimum and maximum measured precipitations are likely to be exceeded in the future.

From the full reconstruction, we calculated precipitation anomalies and identified droughts and pluvials using the two-start two-end definition presented in Section 2.6. Note that these definitions allow for interspersing wet years within a drought and interspersing dry years within a pluvial, but we checked and verified that the average precipitation during each drought was negative, and the average precipitation during each pluvial was positive. We identified one pluvial and seven droughts that lasted 10 years or more (Figure 4b). Only one of these decadal events occurred during the instrumental period, prompting us to look more closely at drought and pluvial duration in the past (Figures 4c and 4d). Droughts typically last longer than pluvials: the mean drought duration is 6 years while the mean pluvial duration is 4 years. Droughts are notably longer before 1900 than after this year, and there is a statistically significant downward trend in drought duration (Figure 4c). Curiously, this decrease in drought duration is not compensated by an increase in pluvial duration (Figure 4d). Upon closer examination, we found that the shortened droughts are closely linked to how droughts are defined. Our definition requires two years of positive precipitation anomalies to end a drought, and the occurrence of these wet-year pairs were less frequent before 1900, resulting in longer droughts, each of which is punctuated by several single wet years (Figures 4b and 4c). After 1900, wet-year pairs occurred more frequently, resulting in shorter droughts and more frequent pluvials, since pluvials are initiated with wet-year pairs (Figures 4b and 4d).

The more frequent occurrences of wet-year pairs is likely a manifest of the wetting trends shown in Figure 4a. While the upward trends in the median and high precipitations are not statistically significant, they likely result in more frequent wet years (thus more frequent wet-year pairs), leading to changes in the duration and frequency of droughts and pluvials. It is a feature, rather than a weakness, of the drought and pluvial definitions that helped detect this shift.

4. Discussion and Conclusions

Using seven tree-ring width chronologies from the Hindu Kush Mountains, we reconstructed five centuries of precipitation history for the Kabul River Basin (Pakistan and Afghanistan). The reconstruction is skillful and robust under rigorous cross-validation. Trend analyses of the reconstruction revealed heterogeneous changes: weak and not significant trends in high and median precipitations, but significant and considerable decline in low precipitations (the left tail of the precipitation distribution). The wetting trends, while not significant, likely led to shifts in the frequency and duration of droughts and pluvials. Prolonged droughts are being replaced by shorter, more frequent ones. Pluvials are occurring more frequently. These heterogeneous trends show that when analyzing hydrological changes, it is important to look at the full distribution shifts, rather than just the mean or median.

19448007, 2022, 24, Downloaded from https://agupubs.onlinelibrary.wiley.com/doi/10.1029/2022GL100703 by Schweizerische Akademie Der, Wiley Online Library on [29/12/2022]. See the Terms and Conditions (https://onlinelibrary.wiley.com/terms-and-conditions) on Wiley Online Library for rules of use; OA articles are governed by the applicable Creative Commons License

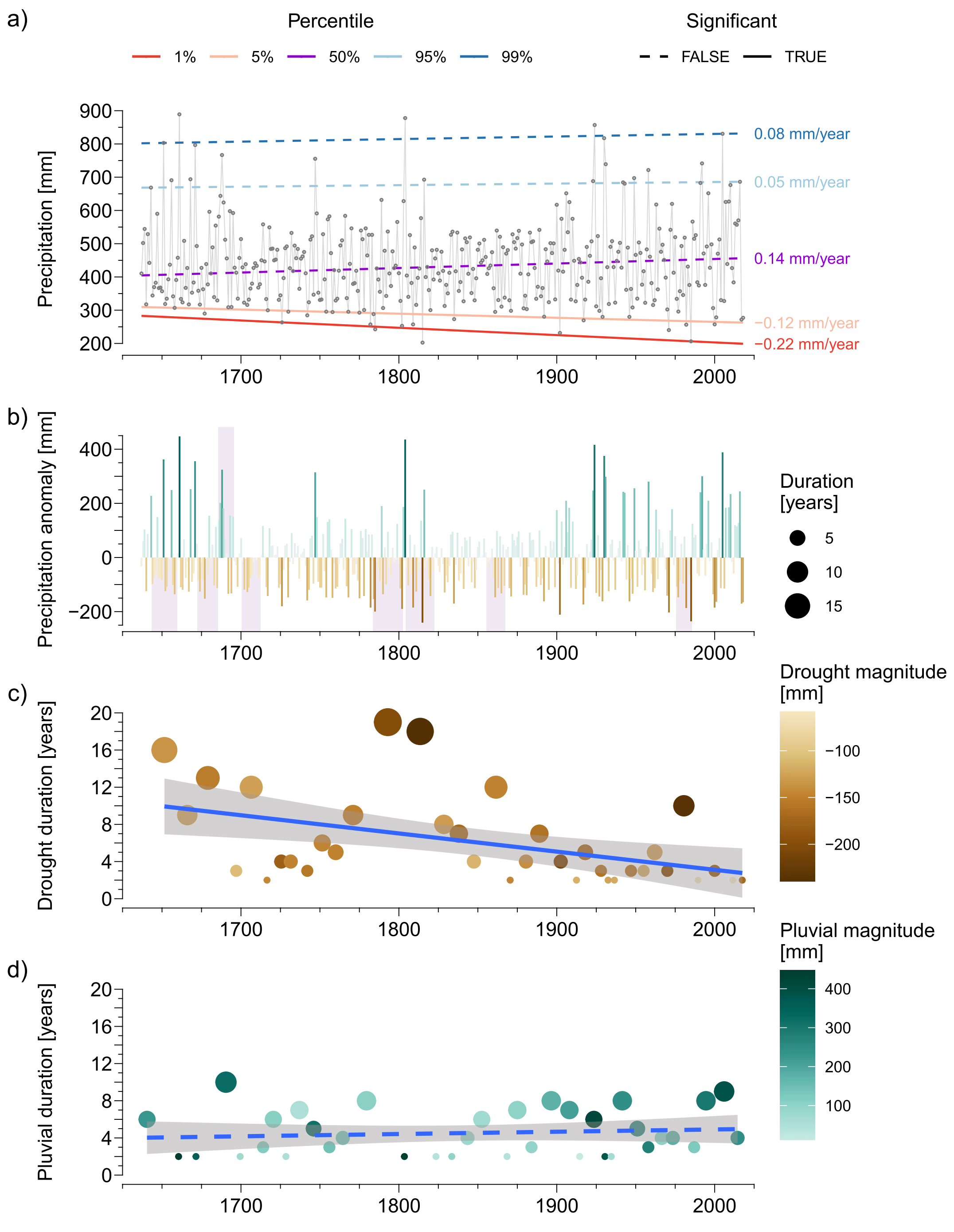

Figure 4. (a) Time series of the full reconstruction, as well as the linear trends in different percentiles, calculated with quantile regression. (b) Time series of precipitation anomalies; highlighted are the droughts and pluvials lasting 10 years or longer. (c) Drought duration over time, with significant downward trend ($p = 0.005$). (d) Pluvial duration over time, with no significant trend ($p = 0.514$). Panels (b–d) share the same color scales, and panels (c and d) the same size scale.

Our reconstruction reveals that dry years are getting drier over the past four centuries, implying increasing drought risks. This result is disconcerting, amidst projections of increased precipitation and floods for the basin as reported in the literature (S. Ahmad et al., 2021). The main moisture source for the basin is western disturbances in the Mediterranean Sea, which have been projected to occur more frequently in the Karakoram (Ridley et al., 2013). Modeling studies involving hydrological models forced with outputs from global circulation models have projected flood intensification for the Kabul River as a whole (Iqbal et al., 2018), but with declining

19448007, 2022, 24, Downloaded from https://agupubs.onlinelibrary.wiley.com/doi/10.1029/2022GL100703 by Schweizerische Akademie Der, Wiley Online Library on [29/12/2022]. See the Terms and Conditions (https://onlinelibrary.wiley.com/terms-and-conditions) on Wiley Online Library for rules of use; OA articles are governed by the applicable Creative Commons License

19448007, 2022, 24, Downloaded from https://agupubs.onlinelibrary.wiley.com/doi/10.1029/2022GL100703 by Schweizerische Akademie Der, Wiley Online Library on [29/12/2022]. See the Terms and Conditions (https://onlinelibrary.wiley.com/terms-and-conditions) on Wiley Online Library for rules of use; OA articles are governed by the applicable Creative Commons License

streamflow for some sub-catchments (Naeem et al., 2013; Shakir et al., 2010). There are still large uncertainties to be resolved in future projections, as discrepancies among climate models have been shown to be greater than calibration uncertainties in hydrological models (Wi et al., 2015).

Even when future uncertainties are resolved and flood intensification turns out to be true, our findings do not contradict such projections, because floods and droughts are not mutually exclusive—floods act on short time scales (hours to months) while droughts manifest on longer time scales (seasons, years, or longer). On the contrary, our results corroborate that the water cycle is intensifying (Huntington, 2006; Seager et al., 2010; Yu et al., 2020), as evidenced by the increased variability in precipitation and more frequent swings between drought and pluvial states.

Our two key findings are inline with those reported by previous studies for the Karakoram region. Beginning with the increase in drought and flood risks, the annual precipitation reconstruction developed by A. Khan et al. (2020), for instance, shows that the frequency of extreme climate events has been rising, with the probability of low and high rainfall years raising by 5% and 8%, respectively. As for the most plausible explanation—the intensification of the water cycle—Treydte et al. (2006) showed that such intensification has already occurred in western Central Asia. Importantly, such change appears to be a long-term trend spanning across a large spatial domain.

Our findings are of concerns for the transboundary management of the Kabul River Basin and, in fact, the entire Indus River system and the countries sharing it. In just a few years, Pakistan has faced drought emergencies (UNCCD, 2022) that have been followed by the 2022 record-breaking floods that displaced 32 million people (Mallapaty, 2022). Facing both flood and drought risks, water management decisions across the Kabul and Indus basins need to consider climate variability at multiple time scales, and tree-ring-based reconstructions is a valuable source of information to serve that need.

Data Availability Statement

NCEP/DOE Reanalysis II (Kanamitsu et al., 2002) and the Global Precipitation Climatology Project (Adler et al., 2018) Monthly Precipitation Climate Data Record data are provided by the NOAA PSL, Boulder, Colorado, USA, from their website at https://psl.noaa.gov. Tree ring and Chitral precipitation data, and the code necessary to reproduce this paper are available on Zenodo (Nguyen, 2022) and can also be cloned from GitHub at https://github.com/ntthung/chitral-precip.

Acknowledgments

Nasrullah Khan's visit to Paolo Cherubini's laboratories was funded by the Swiss National Science Foundation (Grant IZSEZ0_186442). Part of the dendrochronological data were developed during Nasrullah Khan's PhD dissertation work, mentored by Moinuddin Ahmed and Jonathan Palmer, supported by the Higher Education Commission of Pakistan Grant 20-422/R&D (Principal Investigator: Moinuddin Ahmed). Part of the data was developed in a Pak-US joint project (Principal Investigators: Moinuddin Ahmed and Edward Cook), supported by the U.S. Agency for International Development (USAID) NAS Grant PGA-P280423. We thank Jonathan Palmer for his important contributions to the tree ring data. Hung Nguyen is supported by the Lamont-Doherty Postdoctoral Fellowship. The authors thank Boniface Fosu, the editors, and the three anonymous reviewers for their useful suggestions. Our figures made use of colors from https://colorbrewer2.org by Cynthia A. Brewer, Department of Geography, Pennsylvania State University.

References

Adler, R. F., Sapiano, M. R. P., Huffman, G. J., Wang, J.-J., Gu, G., Bolvin, D., et al. (2018). The global precipitation climatology project (GPCP) monthly analysis (new version 2.3) and a review of 2017 global precipitation. *Atmosphere*, *9*(4), 138. https://doi.org/10.3390/atmos9040138

Ahmed, M., Palmer, J., Khan, N., Wahab, M., Fenwick, P., Esper, J., & Cook, E. R. (2011). The dendroclimatic potential of conifers from northern Pakistan. *Dendrochronologia*, *29*(2), 77–88. https://doi.org/10.1016/j.dendro.2010.08.007

Ahmad, S., Jia, H., Chen, Z., Li, Q., Yin, D., Israr, M., et al. (2021). Effects of climate and land use changes on stream flow of Chitral river basin of northern highland Hindu-Kush region of Pakistan. *Journal of Hydro-environment Research*, *38*, 53–62. https://doi.org/10.1016/j.jher.2021.08.001

Ahmad, Z., Hafeez, M., & Ahmad, I. (2012). Hydrology of mountainous areas in the upper Indus Basin, Northern Pakistan with the perspective of climate change. *Environmental Monitoring and Assessment*, *184*(9), 5255–5274. https://doi.org/10.1007/s10661-011-2337-7

Ahmadullah, R., & Dongshik, K. (2015). Assessment of potential dam sites in the Kabul River Basin using GIS. *International Journal of Advanced Computer Science and Applications*, *6*(2), 83–89. https://doi.org/10.14569/IJACSA.2015.060213

Akhtar, S. M., & Iqbal, J. (2017). Assessment of emerging hydrological, water quality issues and policy discussion on water sharing of transboundary Kabul River. *Water Policy*, *19*(4), 650–672. https://doi.org/10.2166/wp.2017.119

Atef, S. S., Sadeqinazhad, F., Farjaad, F., & Amatya, D. M. (2019). Water conflict management and cooperation between Afghanistan and Pakistan. *Journal of Hydrology*, *570*, 875–892. https://doi.org/10.1016/j.jhydrol.2018.12.075

Best, J. (2019). Anthropogenic stresses on the world's big rivers. *Nature Geoscience*, *12*(1), 7–21. https://doi.org/10.1038/s41561-018-0262-x

Bunn, A. G. (2008). A dendrochronology program library in R (dplR). *Dendrochronologia*, *26*(2), 115–124. https://doi.org/10.1016/j.dendro.2008.01.002

Buras, A. (2017). A comment on the expressed population signal. *Dendrochronologia*, *44*, 130–132. https://doi.org/10.1016/j.dendro.2017.03.005

Champion, H. G., Seth, S. K., & Khattak, G. M. (1965). *Forest types of Pakistan*. Pakistan Forest Institute.

Coats, S., Smerdon, J. E., Seager, R., Cook, B. I., & González-Rouco, J. F. (2013). Megadroughts in southwestern North America in ECHO-G Millennial simulations and their comparison to proxy drought reconstructions. *Journal of Climate*, *26*(19), 7635–7649. https://doi.org/10.1175/JCLI-D-12-00603.1

Cook, E. R. (1985). *A time series analysis approach to tree ring standardisation* (PhD Thesis). The University of Arizona.

Cook, E. R., & Kairiukstis, L. A. (Eds.). (1990). *Methods of dendrochronology*. Springer Netherlands. https://doi.org/10.1007/978-94-015-7879-0

Cook, E. R., Palmer, J. G., Ahmed, M., Woodhouse, C. A., Fenwick, P., Zafar, M. U., et al. (2013). Five centuries of Upper Indus River flow from tree rings. *Journal of Hydrology*, *486*, 365–375. https://doi.org/10.1016/j.jhydrol.2013.02.004

Cook, E. R., & Peters, K. (1981). The smoothing spline, a new approach to standardising forest interior tree-ring. *Trre-Ring Bulletin*, *41*, 45–53.

Farinotti, D., Immerzeel, W. W., de Kok, R. J., Quincey, D. J., & Dehecq, A. (2020). Manifestations and mechanisms of the Karakoram glacier anomaly. *Nature Geoscience*, *13*(1), 8–16. https://doi.org/10.1038/s41561-019-0513-5

Forsythe, N., Fowler, H. J., Li, X.-F., Blenkinsop, S., & Pritchard, D. (2017). Karakoram temperature and glacial melt driven by regional atmospheric circulation variability. *Nature Climate Change*, *7*(9), 664–670. https://doi.org/10.1038/nclimate3361

Gudmundsson, L. (2016). Qmap: Statistical transformations for post-processing climate model output. R package version 1.0-4. Retrieved from https://cran.r-project.org/package=qmap

Herweijer, C., Seager, R., Cook, E. R., & Emile-Geay, J. (2007). North American droughts of the last millennium from a gridded network of tree-ring data. *Journal of Climate*, *20*(7), 1353–1376. https://doi.org/10.1175/JCLI4042.1

Hewitt, K. (2005). The Karakoram anomaly? Glacier expansion and the 'elevation effect,' Karakoram Himalaya. *Mountain Research and Development*, *25*(4), 332–340. https://doi.org/10.1659/0276-4741(2005)025[0332:TKAGEA]2.0.CO;2

Higgins, P. A., Palmer, J. G., Rao, M. P., Andersen, M. S., Turney, C. S. M., & Johnson, F. (2022). Unprecedented high Northern Australian streamflow linked to an intensification of the Indo-Australian Monsoon. *Water Resources Research*, *58*(3), e2021WR030881. https://doi.org/10.1029/2021WR030881

Holmes, R. L. (1983). Computer assisted quality control. *Tree-Ring Bulletin*, *43*, 69–78.

Huntington, T. G. (2006). Evidence for intensification of the global water cycle: Review and synthesis. *Journal of Hydrology*, *319*(1), 83–95. https://doi.org/10.1016/j.jhydrol.2005.07.003

Iqbal, M. S., Dahri, Z. H., Querner, E. P., Khan, A., & Hofstra, N. (2018). Impact of climate change on flood frequency and intensity in the Kabul River Basin. *Geosciences*, *8*(4), 114. https://doi.org/10.3390/geosciences8040114

Josse, J., & Husson, F. (2016). missMDA: A package for handling missing values in Multivariate data analysis. *Journal of Statistical Software*, *70*(1), 1–31. https://doi.org/10.18637/jss.v070.i01

Kanamitsu, M., Ebisuzaki, W., Woollen, J., Yang, S.-K., Hnilo, J. J., Fiorino, M., & Potter, G. L. (2002). NCEP–DOE AMIP-II Reanalysis (R-2). *Bulletin of the American Meteorological Society*, *83*(11), 1631–1644. https://doi.org/10.1175/BAMS-83-11-1631

Kapnick, S. B., Delworth, T. L., Ashfaq, M., Malyshev, S., & Milly, P. C. D. (2014). Snowfall less sensitive to warming in Karakoram than in Himalayas due to a unique seasonal cycle. *Nature Geoscience*, *7*(11), 834–840. https://doi.org/10.1038/ngeo2269

Khan, A., Chen, F., Ahmed, M., & Zafar, M. U. (2020). Rainfall reconstruction for the Karakoram region in Pakistan since 1540 CE reveals out-of-phase relationship in rainfall between the southern and northern slopes of the Hindukush-Karakorum-Western Himalaya region. *International Journal of Climatology*, *40*(1), 52–62. https://doi.org/10.1002/joc.6193

Khan, N., Ahmed, M., & Shaukat, S. (2013). Climatic signal in tree-ring chronologies of *Cedrus deodara* from Chitral Hindukush Range of Pakistan. *Geochronometria*, *40*(3), 195–207. https://doi.org/10.2478/s13386-013-0115-8

Khan, N., Ahmed, M., & Wahab, M. (2008). Dendroclimatic potential of Picea smithiana (Wall) Boiss. From Afghanistan. *Pakistan Journal of Botany*, *40*(3), 1063–1070.

Khattak, M. S., Babel, M. S., & Sharif, M. (2011). Hydro-meteorological trends in the upper Indus River basin in Pakistan. *Climate Research*, *46*(2), 103–119. https://doi.org/10.3354/cr00957

Koenker, R. (2005). *Quantile regression*. Cambridge University Press. https://doi.org/10.1017/CBO9780511754098

Laghari, A. N., Vanham, D., & Rauch, W. (2012). The Indus basin in the framework of current and future water resources management. *Hydrology and Earth System Sciences*, *16*(4), 1063–1083. https://doi.org/10.5194/hess-16-1063-2012

Lashkaripour, G. R., & Hussaini, S. A. (2008). Water resource management in Kabul River Basin, eastern Afghanistan. *Environmentalist*, *28*(3), 253–260. https://doi.org/10.1007/s10669-007-9136-2

Mallapaty, S. (2022). Pakistan's floods have displaced 32 million people — Here's how researchers are helping. *Nature*, *609*(7928), 667. https://doi.org/10.1038/d41586-022-02879-2

Maxwell, J. T., Bregy, J. C., Robeson, S. M., Knapp, P. A., Soulé, P. T., & Trouet, V. (2021). Recent increases in tropical cyclone precipitation extremes over the US east coast. *Proceedings of the National Academy of Sciences*, *118*(41), e2105636118. https://doi.org/10.1073/pnas.2105636118

Meko, D., & Graybill, D. A. (1995). Tree-ring reconstruction of upper Gila River discharge. *JAWRA Journal of the American Water Resources Association*, *31*(4), 605–616. https://doi.org/10.1111/j.1752-1688.1995.tb03388.x

Naeem, U. A., Hashmi, H. N., Habib-ur-Rehman, & Shakir, A. S. (2013). Flow trends in river Chitral due to different scenarios of glaciated extent. *KSCE Journal of Civil Engineering*, *17*(1), 244–251. https://doi.org/10.1007/s12205-013-1978-1

Nash, J. E., & Sutcliffe, J. V. (1970). River flow forecasting through conceptual models part I — A discussion of principles. *Journal of Hydrology*, *10*(3), 282–290. https://doi.org/10.1016/0022-1694(70)90255-6

Nguyen, H. T. T. (2022). *ntthung/Chitral-precip: Code for Chitral precipitation reconstruction*. Zenodo. https://doi.org/10.5281/zenodo.6941584

Nguyen, H. T. T., Galelli, S., Xu, C., & Buckley, B. M. (2021). Multi-proxy, multi-season streamflow reconstruction with mass balance adjustment. *Water Resources Research*, *57*(8), e2020WR029394. https://doi.org/10.1029/2020WR029394

Nguyen, H. T. T., Galelli, S., Xu, C., & Buckley, B. M. (2022). Droughts, pluvials, and wet season timing across the Chao Phraya River Basin: A 254-year monthly reconstruction from tree ring widths and δ^{18}O. *Geophysical Research Letters*, *49*(17), e2022GL100442. https://doi.org/10.1029/2022GL100442

Nguyen, H. T. T., Turner, S. W. D., Buckley, B. M., & Galelli, S. (2020). Coherent streamflow variability in monsoon Asia over the past eight centuries—Links to oceanic drivers. *Water Resources Research*, *56*(12), e2020WR027883. https://doi.org/10.1029/2020WR027883

Politis, D. N., & Romano, J. P. (1994). The stationary bootstrap. *Journal of the American Statistical Association*, *89*(428), 1303–1313. https://doi.org/10.1080/01621459.1994.10476870

Raizada, M., & Sahni, K. (1960). Living Indian gymnosperms. Part 1 (Cycades, Ginkgoales and Coniferales). *Indian Forest Records (Botany)*, *5*(2), 73–150.

Ridley, J., Wiltshire, A., & Mathison, C. (2013). More frequent occurrence of westerly disturbances in Karakoram up to 2100. *Science of the Total Environment*, *468–469*, S31–S35. https://doi.org/10.1016/j.scitotenv.2013.03.074

Robeson, S. M., Maxwell, J. T., & Ficklin, D. L. (2020). Bias correction of paleoclimatic reconstructions: A new look at 1,200+ years of upper Colorado river flow. *Geophysical Research Letters*, *47*(1), 1–12. https://doi.org/10.1029/2019GL086689

Sahni, K. C. (1990). *Gymnosperms of India and adjacent countries*. Bishen Singh Mahendra Pal Singh.

Seager, R., Naik, N., & Vecchi, G. A. (2010). Thermodynamic and dynamic mechanisms for large-scale changes in the hydrological cycle in response to global warming. *Journal of Climate*, *23*(17), 4651–4668. https://doi.org/10.1175/2010JCLI3655.1

Shakir, A. S., Rehman, H.-u., & Ehsan, S. (2010). Climate change impact on river flows in Chitral watershed. *Pakistan Journal of Engineering and Applied Sciences*, *7*, 12–23. Retrieved from https://journal.uet.edu.pk/ojs_old/index.php/pjeas/article/view/179

Sharma, B., Amarasinghe, U., Xueliang, C., de Condappa, D., Shah, T., Mukherji, A., et al. (2010). The Indus and the Ganges: River basins under extreme pressure. *Water International*, *35*(5), 493–521. https://doi.org/10.1080/02508060.2010.512996

Singh, G., Kumar, D., & Dash, A. K. (2021). *Pinus gerardiana* Wallichex. D. Don. – A review. *Phytomedicine*, *1*(2), 100024. https://doi.org/10.1016/j.phyplu.2021.100024

19448007, 2022, 24, Downloaded from https://agupubs.onlinelibrary.wiley.com/doi/10.1029/2022GL100703 by Schweizerische Akademie Der, Wiley Online Library on [29/12/2022]. See the Terms and Conditions (https://onlinelibrary.wiley.com/terms-and-conditions) on Wiley Online Library for rules of use; OA articles are governed by the applicable Creative Commons License

Speer, J. H. (2010). *Fundamentals of tree-ring research*. University of Arizona Press.

Stagge, J. H., Rosenberg, D. E., DeRose, R. J., & Rittenour, T. M. (2018). Monthly paleostreamflow reconstruction from annual tree-ring chronologies. *Journal of Hydrology*, *557*, 791–804. https://doi.org/10.1016/j.jhydrol.2017.12.057

Stokes, M. A., & Smiley, T. L. (1996). *An introduction to tree-ring dating*. The University of Arizona Press. Retrieved from https://uapress.arizona.edu/book/an-introduction-to-tree-ring-dating

Taraky, Y. M., McBean, E., Liu, Y., Daggupati, P., Shrestha, N. K., Jiang, A., & Gharabaghi, B. (2021). The role of large dams in a transboundary drought management co-operation framework—Case study of the Kabul River Basin. *Water*, *13*(19), 2628. https://doi.org/10.3390/w13192628

Torbenson, M. C. A., & Stagge, J. H. (2021). Informing seasonal proxy-based flow reconstructions using Baseflow separation: An example from the Potomac River, United States. *Water Resources Research*, *57*(2), e2020WR027706. https://doi.org/10.1029/2020WR027706

Treydte, K. S., Schleser, G. H., Helle, G., Frank, D. C., Winiger, M., Haug, G. H., & Esper, J. (2006). The twentieth century was the wettest period in northern Pakistan over the past millennium. *Nature*, *440*(7088), 1179–1182. https://doi.org/10.1038/nature04743

UNCCD. (2022). *The global land outlook* (Tech. Rep.). United Nations Convention to Combat Desertification. Retrieved from https://www.unccd.int/sites/default/files/2022-04/UNCCD_GLO2_low-res_2.pdf

Wi, S., Yang, Y. C. E., Steinschneider, S., Khalil, A., & Brown, C. M. (2015). Calibration approaches for distributed hydrologic models in poorly gaged basins: Implication for streamflow projections under climate change. *Hydrology and Earth System Sciences*, *19*(2), 857–876. https://doi.org/10.5194/hess-19-857-2015

Wigley, T. M. L., Briffa, K. R., & Jones, P. D. (1984). On the average value of correlated time series, with applications in dendroclimatology and hydrometeorology. *Journal of Applied Meteorology and Climatology*, *23*(2), 201–213. https://doi.org/10.1175/1520-0450(1984)023<0201:OTAVOC>2.0.CO;2

Yao, T., Thompson, L., Yang, W., Yu, W., Gao, Y., Guo, X., et al. (2012). Different glacier status with atmospheric circulations in Tibetan Plateau and surroundings. *Nature Climate Change*, *2*(9), 663–667. https://doi.org/10.1038/nclimate1580

Yousaf, S. (2017). Kabul River and Pak-Afghan relations. *Central Asian Journal*, *80*, 97–112. Retrieved from http://journals.uop.edu.pk/papers/06%20Suliman%20Yousaf.pdf

Yu, L., Josey, S. A., Bingham, F. M., & Lee, T. (2020). Intensification of the global water cycle and evidence from ocean salinity: A synthesis review. *Annals of the New York Academy of Sciences*, *1472*(1), 76–94. https://doi.org/10.1111/nyas.14354

Zafar, M. U., Ahmed, M., Rao, M. P., Buckley, B. M., Khan, N., Wahab, M., & Palmer, J. (2016). Karakorum temperature out of phase with hemispheric trends for the past five centuries. *Climate Dynamics*, *46*(5–6), 1943–1952. https://doi.org/10.1007/s00382-015-2685-z

19448007, 2022, 24, Downloaded from https://agupubs.onlinelibrary.wiley.com/doi/10.1029/2022GL100703 by Schweizerische Akademie Der, Wiley Online Library on [29/12/2022]. See the Terms and Conditions (https://onlinelibrary.wiley.com/terms-and-conditions) on Wiley Online Library for rules of use; OA articles are governed by the applicable Creative Commons License